

Retrieval Pivot Attacks in Hybrid RAG: Measuring and Mitigating Amplified Leakage from Vector Seeds to Graph Expansion

Scott Thornton
scott@perfexion.ai

Abstract—Hybrid Retrieval-Augmented Generation (RAG) pipelines increasingly combine vector similarity search with knowledge graph expansion to support multi-hop reasoning. We show this composition introduces a distinct security failure mode: a semantically retrieved “seed” chunk can pivot via entity linking into sensitive graph neighborhoods, causing data leakage that does not exist in vector-only retrieval. We formalize this risk as Retrieval Pivot Risk (RPR) and define companion metrics Leakage@ k , Amplification Factor (AF), and Pivot Depth (PD) to quantify leakage probability, magnitude, amplification over vector baselines, and structural distance to the first unauthorized node. We further present a taxonomy of four Retrieval Pivot Attacks that exploit the vector-to-graph boundary with injection budgets as small as 10–20 chunks, and we demonstrate that adversarial injection is not required: naturally shared entities (e.g., vendors, infrastructure, compliance standards) create cross-tenant pivot paths organically. In a synthetic multi-tenant enterprise corpus (1,000 documents; 2,785 graph nodes; 15,514 edges) evaluated with 500 queries, the undefended hybrid pipeline exhibits $RPR \approx 0.95$ and $AF(\epsilon) \approx 160\text{--}194\times$ relative to vector-only retrieval, with leakage occurring at $PD = 2$ hops as a structural consequence of the bipartite chunk–entity topology. We validate these findings on the Enron email corpus (50,000 emails; 376,000 graph nodes; 2.3M edges), where undefended hybrid retrieval produces $RPR = 0.695$ on benign queries—lower than the synthetic corpus due to sparser entity connectivity, but still affecting 70% of queries with a mean of 7.1 leaked items each. We propose five layered defenses and find that a single placement fix—per-hop authorization at the graph expansion boundary—eliminates all measured leakage ($RPR \rightarrow 0.0$) across both corpora, all queries, and all attack variants with negligible latency overhead, indicating the vulnerability is primarily a boundary enforcement problem rather than a defense complexity problem.

Index Terms—hybrid RAG, GraphRAG, multi-tenant RAG, access control, data leakage, retrieval security, knowledge graphs, entity linking, composition vulnerabilities

I. INTRODUCTION

Enterprise adoption of Retrieval-Augmented Generation (RAG) has accelerated rapidly: 30–60% of enterprise AI use cases now rely on RAG architectures [1], and the vector database market reached \$1.73 billion in 2024 [2]. To improve multi-hop reasoning over complex organizational knowledge, practitioners increasingly deploy *hybrid* RAG pipelines that combine vector similarity search with knowledge graph expansion [3], [4]. These systems retrieve an initial set of text chunks via embedding similarity, then *pivot* through entity mentions into a knowledge graph to gather structurally related context before passing the assembled results to a large language model

(LLM). We call the transition between vector retrieval and graph expansion the **pivot boundary**: the architectural point where a retrieved seed becomes a graph traversal capability.

This boundary is a *boundary placement* bug. The vector store enforces tenant policy *before* retrieval. The graph expansion must enforce it *again* after entity linking—otherwise an authorized seed chunk becomes an uncontrolled entry point into the knowledge graph. Consider an analyst at an engineering firm who queries about Kubernetes cluster configurations. Vector retrieval returns authorized engineering documents. But those documents mention shared entities (“CloudCorp,” “auth-service”) that also appear in the knowledge graph connected to confidential HR salary records, restricted security credentials, and financial audit data belonging to other tenants. A 2-hop graph expansion traverses through these shared entities into unauthorized neighborhoods, silently injecting sensitive cross-tenant data into the analyst’s context window.

Prior work falls into two separate buckets that do not address this boundary. (1) **Vector-only attacks**: PoisonedRAG achieves 90% attack success rate by injecting 5 malicious texts into vector stores [5]; CorruptRAG [6] and CtrlRAG [7] extend these results. (2) **Graph-only attacks**: GRAGPoisson demonstrates 98% success via relation-centric poisoning within GraphRAG [8]; TKPA [9] and RAG-Safety [10] target graph-side integrity. (3) **The hybrid boundary**—how vector outputs become graph seeds—has not been systematically measured or formalized. The OWASP LLM Top 10 (2025) introduced LLM08 (Vector and Embedding Weaknesses) but does not address graph components [11]. MITRE ATLAS treats RAG as a monolithic system [12]. The SoK on RAG privacy explicitly identifies hybrid RAG security as an open problem [13].

This paper makes three contributions:

- 1) **Composition vulnerability + metrics.** We formalize *Retrieval Pivot Risk (RPR)* and companion metrics (AF, PD, Leakage@ k , severity-weighted leakage) that quantify a compound attack surface emerging from composing two individually secure retrieval modalities. In our bipartite chunk–entity graph, all leakage occurs at $PD = 2$ hops—a structural signature of the pivot boundary (§V).
- 2) **Cross-dataset validation + organic leakage.** We demonstrate the vulnerability on both a synthetic enterprise corpus (1,000 documents, 4 tenants) and the Enron

email corpus (50,000 emails, 5 departments), showing $RPR = 0.95$ and $RPR = 0.70$ respectively without adversarial injection. We present four Retrieval Pivot Attacks (A1–A4) exploiting the pivot boundary with injection budgets of 10–20 chunks (§IV, §VII).

3) **Defense placement analysis.** We evaluate five layered defenses (D1–D5) and show that authorization must be re-checked at the graph expansion boundary. D1 (per-hop authorization) alone eliminates all measured leakage ($RPR \rightarrow 0.0$) across both corpora, all queries, all attack variants, and metadata mislabel rates up to 5%. D2–D5 serve as utility optimizers and defense-in-depth layers (§VIII, §VII).

The complete codebase, data generators, attack implementations, defense suite, and experimental results are available at <https://github.com/scthornton/hybrid-rag-pivot-attacks>.

II. BACKGROUND

A. Vector Retrieval in RAG

Standard RAG systems encode documents as dense vector embeddings using models such as all-MiniLM-L6-v2 [14] and retrieve the top- k chunks by cosine similarity to the query embedding. In multi-tenant deployments, vector stores apply metadata prefilters (e.g., tenant ID) before similarity search, ensuring that retrieval respects organizational boundaries. This prefiltering makes vector-only RAG robust against cross-tenant leakage: our experiments confirm $RPR = 0.0$ for vector-only pipelines across all evaluation queries on both synthetic and Enron corpora (§VII).

B. Knowledge Graph RAG

GraphRAG [4] and related approaches construct knowledge graphs from document corpora via named entity recognition (NER) and relation extraction, then leverage graph structure for multi-hop reasoning. Systems like AgCyRAG [15] use LLM-driven graph traversal for complex queries. Graph-based retrieval provides superior comprehensiveness on multi-hop queries—86% versus 57% for vector RAG [3]—but introduces graph-specific attack surfaces: GRAGPoison [8] achieves 98% attack success through relation-centric poisoning, and TKPA [9] drops QA accuracy from 95% to 50% by modifying just 0.06% of corpus text.

C. Hybrid RAG and the Pivot Boundary

Hybrid RAG combines both retrieval modalities in a pipeline:

- 1) **Vector retrieval:** Query embedding \rightarrow cosine similarity \rightarrow top- k seed chunks $S(q)$.
- 2) **Entity linking:** Extract named entities from $S(q)$ via NER; map entity mentions to knowledge graph node IDs.
- 3) **Graph expansion:** BFS/DFS traversal from linked entity nodes to depth d , gathering structurally related nodes.
- 4) **Context merge:** Combine vector-retrieved chunks with graph-expanded context for LLM generation.

We define the **pivot boundary** as the transition between steps 1–2 and steps 3–4: the point where vector retrieval results become graph traversal seeds. This boundary is the attack surface we study. Vector-side prefilters operate *before* the pivot; graph expansion operates *after* it. If graph expansion does not independently enforce access controls, any entity mentioned in an authorized seed chunk becomes an uncontrolled entry point into the knowledge graph.

Running example. Consider an INTERNAL-clearance engineer at Acme Corp who queries “What infrastructure does auth-service depend on?” The vector store returns authorized Acme engineering documents mentioning auth-service. Entity linking maps “auth-service” to a shared entity node in the knowledge graph. BFS expansion then walks: auth-service \rightarrow CloudCorp (shared vendor entity, hop 1) \rightarrow Umbrella Security’s CONFIDENTIAL incident-response documents (hop 2). The engineer’s authorized query silently pulls CONFIDENTIAL cross-tenant data into the context—a 2-hop pivot through a legitimate shared entity.

III. THREAT MODEL

A. System Model

We consider a multi-tenant enterprise hybrid RAG system with the following components:

- A **vector store** (ChromaDB) containing document chunk embeddings with tenant and sensitivity metadata.
- A **knowledge graph** (Neo4j) containing entity nodes, chunk nodes, and typed edges (MENTIONS, DEPENDS_ON, BELONGS_TO, RELATED_TO) extracted from the document corpus.
- An **entity linker** that maps NER-extracted entities from vector-retrieved chunks to graph node IDs.
- A **graph expander** that performs BFS traversal from linked entities to depth d (default $d = 2$), implemented via Neo4j’s apoc.path.spanningTree for hop-distance tracking.
- Four organizational **tenants** with distinct data ownership boundaries.
- Four **sensitivity tiers**: PUBLIC ($\approx 40\%$ of corpus), INTERNAL (30%), CONFIDENTIAL (20%), RESTRICTED (10%).

B. Attacker Capabilities

We consider two attacker models:

Injection attacker. The attacker holds a legitimate account in one tenant (acme_engineering) and can inject documents into the shared corpus through standard channels—wiki edits, ticket updates, shared document repositories. Injected documents undergo normal ingestion: chunking, NER-based entity extraction, embedding, and indexing into both vector and graph stores. The attacker’s injection budget is modest: 10–20 chunks, consistent with the budgets shown effective in prior work [5], [6].

No-injection attacker. The attacker holds a legitimate account and crafts queries that mention bridge entities (shared infrastructure names, vendor references, cross-team personnel)

to maximize pivot probability through naturally occurring cross-tenant entity connections. This attacker requires *zero document injection*—the organic structure of the multi-tenant knowledge graph provides the pivot paths. Our evaluation shows that this attacker model achieves $RPR = 0.95$ through benign queries alone (§VII), demonstrating that the vulnerability is *structural* rather than injection-dependent.

C. Attacker Goals

- **G1: Cross-tenant access.** Cause the retrieval context for a query in the attacker’s tenant to include chunks or entities belonging to other tenants.
- **G2: Sensitivity escalation.** Cause an INTERNAL clearance user’s context to include CONFIDENTIAL or RESTRICTED items.
- **G3: Amplified leakage.** Achieve leakage in the hybrid pipeline that exceeds what is possible with vector-only retrieval (i.e., $AF > 1$).

D. Adaptive Attacker Considerations

An adaptive attacker aware of D1 (per-hop authorization) might attempt to bypass it through: (a) **metadata spoofing**—forging tenant or sensitivity labels during document injection, or (b) **same-tenant escalation**—crafting documents within the attacker’s own tenant that link to higher-sensitivity content within the same tenant boundary. D1 is robust against (a) if and only if the ingestion pipeline enforces metadata integrity (the metadata is assigned by the system, not the uploader). We evaluate D1’s robustness under metadata corruption in §VII-K and discuss mitigation strategies in §VIII-B. Same-tenant escalation (b) targets *sensitivity* boundaries rather than *tenant* boundaries and requires the attacker to already have write access to the target tenant’s corpus.

E. Metadata Integrity Assumption

D1 (per-hop authorization) relies on node metadata—tenant labels and sensitivity tiers—being trustworthy. **We assume metadata is system-assigned during document ingestion** (the uploader cannot choose tenant or sensitivity labels). If an attacker can forge metadata, D1 can be bypassed. We evaluate robustness under random metadata corruption in §VII-K and discuss additional integrity mechanisms in §VIII-B.

F. Scope

We measure unauthorized items in the retrieval context window, not exfiltrated tokens or generated text. We focus exclusively on the retrieval layer. We do not evaluate LLM generation quality, jailbreaking, or prompt injection. The attacker does not have direct database access, cannot modify model weights, and cannot alter the pipeline configuration. We omit a graph-only baseline (P2) because graph-only RAG without vector seeding is a fundamentally different retrieval paradigm—our question is *amplification created by composition*, not graph-only security, which is addressed by prior work [8], [9].

IV. RETRIEVAL PIVOT ATTACKS

We define four non-adaptive attacks (A1–A4) that exploit the pivot boundary with increasing structural sophistication, and three adaptive attacks (A5–A7) that target the defense mechanisms themselves. Each attack operates within the threat model of §III: the attacker injects a small number of crafted documents that undergo standard ingestion.

A. A1: Seed Steering

Objective. Maximize the probability that attacker-crafted chunks are retrieved by target queries while embedding entity mentions that link to sensitive graph neighborhoods.

Mechanism. The attacker estimates the query centroid for target query families (e.g., “infrastructure monitoring”) and crafts 10 chunks with high semantic overlap to this centroid. Each chunk embeds 2 pivot entities—entities that are within 1–2 hops of sensitive nodes in the knowledge graph (e.g., `k8s-prod-cluster`, `auth-service`). Chunks are labeled PUBLIC with low provenance scores (0.3) to bypass any trust-based filtering. When retrieved, entity linking maps the embedded entity mentions to graph nodes, seeding expansion into sensitive neighborhoods.

Entry point. Vector retrieval (cosine similarity).

Pivot mechanism. Entity linking from retrieved chunk to graph node.

B. A2: Entity Anchor Injection

Objective. Force entity linking to create dense connections between injected chunks and sensitive graph neighborhoods.

Mechanism. The attacker identifies anchor entities adjacent to sensitive nodes (e.g., entities 1 hop from restricted credentials) and crafts chunks with dense entity mentions: 3+ mentions of the primary target entity per chunk, plus 2 related entities. NER extraction creates MENTIONS edges from each chunk to the target entities. Any query that retrieves one of these chunks—even incidentally—triggers graph expansion toward the sensitive area.

Entry point. Entity extraction during ingestion.

Pivot mechanism. MENTIONS edges from chunk to target entity nodes.

C. A3: Neighborhood Flooding

Objective. Inflate the local density around a target entity to increase the volume of sensitive content reachable through BFS expansion.

Mechanism. The attacker injects 20 chunks, each mentioning a high-value target entity near a sensitive subgraph. Each chunk also mentions a different neighbor entity, creating a dense web of edges. The result is a “graph gravity well”: the target entity accumulates many more edges than the graph average, causing BFS expansion to gather a larger neighborhood when traversing through this entity. Note that our pipeline uses uniform BFS traversal (not degree-weighted or PageRank-based expansion), so the flooding increases reachable volume rather than biasing traversal order.

Algorithm 1 General Retrieval Pivot Attack

Require: Target query family \mathcal{Q}_T , injection budget B , pivot entities E_p , target neighborhood N_T

Ensure: Injected chunks C_{atk}

- 1: **for** $i = 1$ to B **do**
- 2: $c_i \leftarrow \text{CRAFTCHUNK}(\mathcal{Q}_T, E_p)$ \triangleright High similarity to \mathcal{Q}_T
- 3: $c_i.\text{entities} \leftarrow \text{EMBEDENTITIES}(E_p, N_T)$ \triangleright Mentions near N_T
- 4: $c_i.\text{sensitivity} \leftarrow \text{PUBLIC}$
- 5: $c_i.\text{provenance} \leftarrow 0.3$
- 6: $C_{\text{atk}} \leftarrow C_{\text{atk}} \cup \{c_i\}$
- 7: **end for**
- 8: **INGEST**(C_{atk}) \triangleright Standard pipeline: chunk, NER, embed, index
- 9: **return** C_{atk}

Entry point. Graph topology manipulation via ingestion.

Pivot mechanism. Inflated local density increases BFS expansion volume.

D. A4: Bridge Node Attack

Objective. Create artificial cross-tenant edges that enable graph traversal from the attacker’s tenant into a target tenant.

Mechanism. The attacker crafts 15 chunks that co-mention entities from both the attacker’s tenant and the target tenant within the same document. NER extraction creates entity nodes on both sides of the tenant boundary, and relation extraction creates RELATED_TO edges between them. After ingestion, BFS expansion from the attacker’s authorized subgraph can traverse these artificial bridge edges into the target tenant’s data.

Entry point. Cross-tenant entity co-mention.

Pivot mechanism. Artificial RELATED_TO edges spanning tenant boundaries.

Algorithm 1 formalizes the general pivot attack framework.

V. METRICS

We introduce metrics to quantify retrieval pivot risk. Let q denote a query, u a user with tenant t_u and clearance level ℓ_u , $S_k(q)$ the top- k context set, and $\text{Sensitive}(x, u)$ a predicate that is true when item x has sensitivity $> \ell_u$ or tenant $\neq t_u$ (entity nodes with empty-string tenants are excluded from cross-tenant counts, as they are tenant-neutral shared concepts—not leaked items themselves but rather the pivot bridges through which leakage propagates). Let $\text{Seeds}(q) \subseteq S_k(q)$ denote the set of entity nodes that are linked from vector-retrieved chunks via NER extraction—these are the graph entry points that initiate BFS expansion.

Item serialization. Each *item* in $S_k(q)$ is a node serialized for the LLM context: chunk nodes are serialized as their source text; entity nodes are serialized as `{name, type, top-3 relations}`. Context size counts the total number of serialized nodes (chunks + entities) presented to the LLM.

TABLE I: Notation summary.

Symbol	Definition
q	Query
u	User with tenant t_u and clearance ℓ_u
$S_k(q)$	Top- k context set (serialized items)
$\text{Seeds}(q)$	Entity nodes linked from vector-retrieved chunks
$\text{Sensitive}(x, u)$	x has $\ell_x > \ell_u$ or $t_x \neq t_u$
RPR	Prob. of any sensitive item in context
Leakage@ k	Count of sensitive items in context
SWL	Severity-weighted leakage
AF(ϵ)	Leakage ratio: hybrid / max(vector, ϵ)
PD	Min hops from seed to first sensitive node

The default pipeline configuration (depth $d = 2$, branching ≤ 10 , total ≤ 100 nodes, top- $k=10$ vector results) produces ~ 110 items per query in the undefended hybrid pipeline (P3). Table I summarizes the notation used throughout.

A. Retrieval Pivot Risk (RPR)

RPR measures the probability that a query’s retrieval context contains any unauthorized item:

$$\text{RPR}(u) = \Pr_{q \sim \mathcal{Q}} [\exists x \in S_k(q) : \text{Sensitive}(x, u)] \quad (1)$$

RPR is operationalized as the fraction of evaluation queries whose context contains at least one sensitive item. We report RPR with 95% bootstrap confidence intervals (10,000 resamples).

B. Leakage@ k

Leakage@ k counts the number of unauthorized items in the context:

$$\text{Leakage}@k(q, u) = |\{x \in S_k(q) : \text{Sensitive}(x, u)\}| \quad (2)$$

While RPR captures *whether* leakage occurs, Leakage@ k captures its *severity*. A context with 1 leaked item and one with 20 both yield RPR = 1, but their Leakage@ k values differ by 20 \times .

C. Severity-Weighted Leakage

Not all leakage is equally harmful. A PUBLIC-clearance user receiving INTERNAL content is a lesser violation than receiving RESTRICTED content. We define severity-weighted leakage as:

$$\text{SWL}(q, u) = \sum_{\substack{x \in S_k(q) \\ \text{Sensitive}(x, u)}} w(x, u) \quad (3)$$

where the per-item weight $w(x, u)$ captures two distinct policy violations:

$$w(x, u) = \begin{cases} \ell_x - \ell_u & \text{if } \ell_x > \ell_u \\ 1 & \text{if } t_x \neq t_u \wedge \ell_x \leq \ell_u \end{cases} \quad (4)$$

Here ℓ_x is the sensitivity level (PUBLIC=0, INTERNAL=1, CONFIDENTIAL=2, RESTRICTED=3) and t_x the tenant of

item x . Over-clearance items contribute weight proportional to the sensitivity gap. Cross-tenant items that do not exceed the user’s clearance receive a penalty of 1, reflecting the policy violation of accessing another tenant’s data regardless of sensitivity. In our experiments, the INTERNAL-clearance user observing RESTRICTED items produces weight 2 per item, CONFIDENTIAL produces weight 1, and cross-tenant PUBLIC items produce weight 1.

D. Amplification Factor

AF quantifies the leakage increase that hybrid retrieval introduces compared to vector-only retrieval:

$$AF = \frac{\mathbb{E}[\text{Leakage}@k]_{\text{hybrid}}}{\mathbb{E}[\text{Leakage}@k]_{\text{vector}}} \quad (5)$$

When the vector baseline produces zero leakage (which our experiments confirm), $AF = \infty$ for any nonzero hybrid leakage. To provide a finite, plottable alternative, we also report $AF(\epsilon)$:

$$AF(\epsilon) = \frac{\mathbb{E}[\text{Leakage}@k]_{\text{hybrid}}}{\max(\mathbb{E}[\text{Leakage}@k]_{\text{vector}}, \epsilon)} \quad (6)$$

with $\epsilon = 0.1$, alongside the absolute difference $\Delta\text{Leakage} = \mathbb{E}[\text{Leakage}@k]_{\text{hybrid}} - \mathbb{E}[\text{Leakage}@k]_{\text{vector}}$.

Because the vector-only baseline produces zero leakage in our setting, ratio metrics can be ill-conditioned ($AF = \infty$). We therefore use $\Delta\text{Leakage}$ as the primary magnitude measure and $AF(\epsilon)$ only as a secondary, plottable indicator. The central security finding is not the exact amplification ratio but that hybridization **creates nonzero leakage** despite secure vector prefiltering.

E. Pivot Depth (PD)

PD measures the minimum graph distance from a seed node to the first sensitive node reached during expansion:

$$PD(q) = \min\{d(s, x) : s \in \text{Seeds}(q), x \in S_k(q), \text{Sensitive}(x, u)\} \quad (7)$$

where $d(s, x)$ is the shortest-path distance in the knowledge graph from seed s to node x , computed via `apoc.path.spanningTree` which yields paths with explicit hop counts. We report PD as a distribution (min, median, max) across queries that exhibit leakage, rather than a single summary statistic. Operationally, PD identifies the *minimum traversal depth at which enforcement must occur*: if all leakage has $PD = d$, limiting expansion to depth $< d$ or inserting an authorization check at depth d is sufficient to prevent it.

VI. EXPERIMENTAL SETUP

A. Synthetic Enterprise Corpus

We generate a multi-tenant enterprise corpus of 1,000 documents across four organizational tenants: `acme_engineering`, `globex_finance`, `initech_hr`, and `umbrella_security`. Documents are produced by 12 domain-specific generators (3 per tenant) that

embed realistic entity mentions—system names, personnel, projects, compliance standards—using curated entity pools.

Sensitivity tiers follow a realistic distribution: PUBLIC (40%), INTERNAL (30%), CONFIDENTIAL (20%), and RESTRICTED (10%). Each document includes ground-truth entity annotations and sensitivity labels.

Bridge entities. We inject 15 bridge entities across 5 categories (shared vendors, shared infrastructure, shared personnel, shared compliance standards, and shared projects) that naturally appear in documents across multiple tenants. For example, “CloudCorp” appears in both engineering and finance documents, and “auth-service” appears in both engineering and security documents. After NER-based entity extraction, the knowledge graph contains 40 naturally shared entities across tenant boundaries—not through adversarial injection, but through legitimate cross-team references that any multi-tenant organization would exhibit.

B. Knowledge Graph Construction

Documents undergo chunking (300-token windows, 50-token overlap), producing $\sim 2,000$ chunks from 1,000 source documents (average ~ 2 chunks per document). Chunks are processed through spaCy NER extraction (`en_core_web_sm`), two-pass relation extraction (ground-truth relation resolution followed by pattern-based extraction across 5 typed relations: `DEPENDS_ON`, `OWNED_BY`, `BELONGS_TO`, `CONTAINS`, `DERIVED_FROM`, plus `RELATED_TO` fallback), and embedding via all-MiniLM-L6-v2 (384 dimensions). The resulting knowledge graph contains 2,785 nodes (785 entity nodes + 2,000 chunk nodes) and 15,514 edges (7,386 extracted relations plus `MENTIONS`, `CONTAINS`, and `BELONGS_TO` structural edges added during graph construction).

C. Enron Email Corpus

To validate that Retrieval Pivot Risk is not an artifact of synthetic construction, we evaluate on the Enron email corpus—a public-record dataset of $\sim 500,000$ corporate emails from ~ 150 Enron employees, released during the 2001 FERC investigation. We subsample to 50,000 emails from the most active employees and assign tenants based on departmental structure:

- `trading` — Trading, West/East Power Trading
- `legal` — Legal, Government Affairs
- `finance` — Finance, Risk Management, Accounting
- `energy_services` — Energy Services, Pipeline, ENA
- `executive` — Executive, Office of the Chairman

Sensitivity labels are assigned by keyword matching: RESTRICTED (attorney-client privilege markers, password shares, strategy memos), CONFIDENTIAL (deal negotiations, valuations, board communications), INTERNAL (standard departmental communications), PUBLIC (company-wide announcements). The resulting distribution (92% PUBLIC, 6.7% CONFIDENTIAL, 0.7% RESTRICTED, 0.3% INTERNAL) is

TABLE II: Pipeline variants and their defense configurations.

ID	Pipeline	Defenses
P1	Vector-only	Tenant prefilter
P3	Hybrid baseline	None
P4	Hybrid + D1	Per-hop authz
P5	Hybrid + D1,D2	+ Edge allowlist
P6	Hybrid + D1–D3	+ Budgeted traversal
P7	Hybrid + D1–D4	+ Trust weighting
P8	Hybrid + D1–D5	+ Merge filter

skewed compared to the synthetic corpus—reflecting realistic email traffic where most messages are routine.

Chunking (300-token windows, 50-token overlap) produces 152,064 chunks. spaCy NER extraction (`en_core_web_sm`) identifies 2.07M entity mentions. The resulting knowledge graph contains 376,000 nodes (174,000 entity nodes + 152,000 chunk nodes + 50,000 document nodes) and 2.3M edges. Nineteen entities are naturally shared across departmental boundaries—cross-department executives (Ken Lay, Jeff Skilling, Andy Fastow), external organizations (Arthur Andersen, Vinson & Elkins), deal names (Project Raptor, LJM2), and internal systems (EnronOnline).

Key differences from synthetic. The Enron graph is $135\times$ larger than the synthetic graph (376K vs. 2.8K nodes) but has fewer intentional bridge entities (19 vs. 40). Email text produces noisier NER extractions (dates, monetary amounts, partial names) than curated synthetic documents, creating more spurious entity connections but also more entity fragmentation. These properties make the Enron corpus a stress test for whether the pivot vulnerability generalizes beyond controlled conditions.

D. Pipeline Variants

We evaluate 7 pipeline configurations (Table II): We omit a graph-only baseline (P2) because graph-only retrieval without vector seeding is a fundamentally different paradigm that does not involve the pivot boundary under study. Its security properties are addressed by prior work on GraphRAG attacks [8], [9].

E. Evaluation Protocol

Synthetic corpus. We evaluate each pipeline on 500 template-generated queries: 350 benign queries (standard domain questions stratified across 4 tenants and 3 clearance levels) and 150 adversarial queries (queries that mention bridge entities or target cross-tenant pivot paths, stratified across attack types A1–A4). The evaluation user belongs to `acme_engineering` with INTERNAL clearance.

Enron corpus. We evaluate P1, P3, and P4 on 200 queries (100 benign + 100 adversarial) generated from department-specific templates. The evaluation user belongs to `trading` with INTERNAL clearance.

For each query, we measure RPR, Leakage@k, severity-weighted leakage, $AF(\epsilon)$, Δ Leakage, PD distribution, latency, and context size. All RPR and Leakage@k val-

ues are reported with 95% bootstrap confidence intervals (10,000 resamples, seed 42). Graph expansion uses `apoc.path.spanningTree` for BFS with hop-distance tracking: each expanded node records its minimum distance from the nearest seed, enabling precise PD measurement.

Statistical methodology. All metrics are reported with 95% bootstrap confidence intervals (10,000 resamples, percentile method, seed 42). We use non-parametric bootstrap because RPR values near 0 or 1 violate normal approximations, and leakage distributions are highly skewed. Our query sets (500 synthetic, 200 Enron) each provide power > 0.80 for detecting 5pp differences (Appendix D provides sample size justification, multiple comparison corrections, and ϵ sensitivity analysis).

Reproducibility. All experiments use a single fixed random seed (42) for corpus generation, query sampling, and bootstrap resampling. Pipeline configurations are built programmatically (not from YAML) to ensure parameter consistency across variants. Appendix A provides the full reproduction sequence; Appendix D details the corpus generator; Appendix D lists all query templates. The codebase includes 255 passing unit tests.

F. Attack Evaluation

We evaluate all four attacks (A1–A4) against the undefended hybrid pipeline (P3) and three defense configurations (P4, P6, P8). For each attack, payloads are injected into a clean corpus, and 10 adversarial queries are executed against each pipeline variant. After each attack evaluation, the graph is rebuilt from the clean corpus to prevent cross-contamination between attack experiments.

VII. RESULTS

A. Hybrid RAG Amplifies Leakage

Table III presents security metrics across all pipeline variants. The central finding is stark: **the undefended hybrid pipeline (P3) leaks massively while the vector-only baseline (P1) leaks nothing.**

P1 achieves $RPR = 0.0$ on both query sets—the vector store’s tenant prefilter prevents any cross-tenant or sensitivity-escalated content from reaching the context. In contrast, P3 achieves $RPR = 0.954$ [95% CI: 0.931, 0.974] on 350 benign queries (334 of 350 queries produce leakage) and $RPR = 0.947$ [0.907, 0.980] on 150 adversarial queries (142 of 150 queries leak). Mean $Leakage@k$ reaches 16.0 items for benign queries and 19.4 for adversarial queries—meaning that roughly 15–18% of the 110-item context consists of unauthorized content. Severity-weighted leakage averages 22.9 (benign) and 26.4 (adversarial), indicating that leaked items skew toward higher sensitivity tiers.

Because the vector baseline (P1) produces zero leakage, the absolute difference Δ Leakage = 16.0 (benign) and 19.4 (adversarial) is the most direct measure of the hybrid penalty: each query exposes 16–19 additional unauthorized items purely from graph expansion. The classical Amplification Factor is formally $AF = \infty$ (division by zero); the regularized

TABLE III: Defense ablation: security metrics across pipeline variants (500 queries: 350 benign + 150 adversarial). RPR = Retrieval Pivot Risk with 95% bootstrap CI, Leak = mean Leakage@k, SWL = severity-weighted leakage, PD = Pivot Depth (hops), Ctx = mean context size. “–” indicates no leakage occurred (PD undefined).

Variant	Benign Queries (n = 350)					Adversarial Queries (n = 150)				
	RPR [CI]	Leak	SWL	PD	Ctx	RPR [CI]	Leak	SWL	PD	Ctx
P1 (Vector)	0.000	0.0	0.0	–	10	0.000	0.0	0.0	–	10
P3 (Hybrid)	.954 [.931,.974]	16.0	22.9	2.0	110	.947 [.907,.980]	19.4	26.4	2.0	110
P4 (+D1)	0.000	0.0	0.0	–	56	0.000	0.0	0.0	–	50
P5 (+D1,D2)	0.000	0.0	0.0	–	57	0.000	0.0	0.0	–	51
P6 (+D1-D3)	0.000	0.0	0.0	–	29	0.000	0.0	0.0	–	28
P7 (+D1-D4)	0.000	0.0	0.0	–	28	0.000	0.0	0.0	–	24
P8 (All)	0.000	0.0	0.0	–	20	0.000	0.0	0.0	–	20

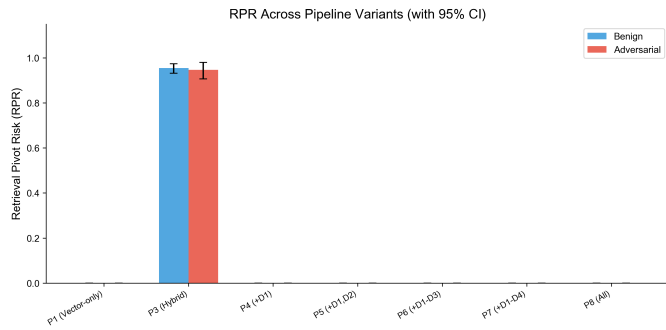


Fig. 1: Retrieval Pivot Risk with 95% bootstrap CIs across pipeline variants. P3 (undefended hybrid) shows RPR ≈ 0.95 . All defended variants (P4–P8) achieve RPR = 0.0.

variant $AF(\epsilon=0.1) = 160\text{--}194\times$ provides a finite proxy.¹ The hybrid architecture does not merely amplify existing risk—it creates risk from nothing: P1 achieves RPR = 0.0 while P3 reaches RPR = 0.95 on identical queries.

Figure 1 shows RPR with bootstrap confidence intervals across pipeline variants.

B. The $PD = 2$ Structural Signature

All leakage in P3 occurs at exactly $PD = 2$ hops: the PD distribution is ($\min = 2$, $\text{median} = 2$, $\max = 2$) across all 476 leaking queries. This uniformity is not coincidental—it is a structural consequence of the bipartite chunk-entity graph topology in our construction. The pivot path is:

- 1) **Hop 0:** Authorized seed chunk (retrieved by vector similarity, passes tenant prefilter).
- 2) **Hop 1:** Shared entity node (linked via NER from seed chunk text; entity nodes carry no tenant ownership).
- 3) **Hop 2:** Unauthorized chunk (connected to the shared entity via MENTIONS edge; belongs to a different tenant or higher sensitivity tier).

This 2-hop pattern is inherent to any hybrid RAG system that constructs a bipartite graph between chunks and entities with expansion depth $d \geq 2$: the entity-linking step creates a

¹ $AF(\epsilon)$ is sensitive to the choice of ϵ ; see Appendix D for a robustness check across $\epsilon \in \{0.01, 0.05, 0.1, 0.5\}$.

TABLE IV: Organic leakage by bridge entity category under P3 (no injection). Queries = leaking queries with that bridge type at hop 1. Leak = attributed leaked items.

Bridge Category	Benign		Adversarial	
	Queries	Leak	Queries	Leak
Personnel	104	1,321	67	1,244
Compliance	46	782	33	489
Infrastructure	43	406	16	213
Vendor	0	0	30	218
Project	7	87	24	228
(No bridge at hop 1)	175	—	22	—
Total leaking	334	5,595	142	2,907

structural bridge between vector-retrieved content and graph-stored content. The $PD=2$ finding is *structural in our bipartite construction*—knowledge graphs with richer entity-to-entity relationships (e.g., ontological hierarchies, multi-hop inference chains) may exhibit leakage at deeper pivot depths. We discuss how PD varies with traversal parameters in §VII-I.

C. Organic Leakage: No Injection Required

A critical observation from our 350 benign queries is that RPR = 0.954 *without any adversarial injection*. The 40 naturally shared entities across tenant boundaries—shared infrastructure, vendors, personnel, compliance standards, and projects—provide sufficient pivot paths for massive leakage through ordinary queries. In our corpus, 334 of 350 benign queries (95.4%) trigger cross-tenant leakage through organic entity connections. This means the vulnerability is *structural*: it exists in any multi-tenant hybrid RAG deployment where tenants share real-world entities, regardless of whether an attacker injects content.

Bridge category analysis. To understand which types of shared entities drive leakage, we analyze the hop-1 pivot nodes in each leaking query’s traversal path and classify them against the 5 bridge entity categories (Table IV).

Personnel entities (shared employees like “Maria Chen”) dominate: they appear at hop 1 in 31% of benign leaking queries and 47% of adversarial leaking queries, accounting for 23.6% and 42.8% of attributed leakage respectively. Compliance entities (SOC2, PCI-DSS, ISO27001) rank second.

TABLE V: Connectivity sweep: effect of bridge entity count on P3 RPR and mean Leakage@k. RPR is remarkably stable; mean leakage increases monotonically with connectivity.

Bridges	P3 RPR	Mean Leak	PD
0	0.93	21.5	2.0
5	0.95	26.6	2.0
10	0.95	30.5	2.0
15	0.95	31.5	2.0
25	0.95	32.5	2.0
40	0.94	34.5	2.0

TABLE VI: Embedding model sensitivity: P3 RPR and mean Leakage@k across two embedding models. The vulnerability persists regardless of embedding quality.

Model	Benign		Adversarial	
	RPR	Leak	RPR	Leak
MiniLM-L6 (384d)	0.954	16.0	0.947	19.4
MPNet (768d)	0.994	19.4	0.980	28.4

Notably, 52% of benign leaking queries have *no recognized bridge entity* at hop 1—non-bridge entities (monetary amounts, dates, generic organizational terms extracted by spaCy NER) also create unintended cross-tenant paths, indicating that the leakage risk is broader than just named shared entities.

D. Connectivity Sensitivity

To measure how shared-entity density affects leakage, we regenerate the corpus with bridge entity counts $\in \{0, 5, 10, 15, 25, 40\}$, rebuild all indexes for each count, and run 100 adversarial queries through P3 (Table V).

Two findings emerge. First, **RPR is remarkably stable (0.93–0.95) regardless of bridge count**—even with zero intentional bridge entities, organic entity overlap from spaCy NER produces RPR = 0.93. Second, **mean leakage scales monotonically** from 21.5 (0 bridges) to 34.5 (40 bridges), a 60% increase. Bridge entities do not *enable* leakage (BFS already reaches cross-tenant nodes through generic NER entities), but they *amplify* the volume of leaked content per query. PD remains uniformly 2.0 across all bridge counts, confirming the structural bipartite pivot.

E. Embedding Model Sensitivity

To verify that the pivot vulnerability is structural rather than embedding-dependent, we repeat the P1 and P3 evaluations using all-mpnet-base-v2 (768 dimensions, higher retrieval quality) in addition to our default all-MiniLM-L6-v2 (384 dimensions). We rebuild the ChromaDB collection for each model and run the full 500-query evaluation (Table VI).

The higher-quality MPNet model actually *increases* RPR: from 0.954 to 0.994 on benign queries, and from 0.947 to 0.980 on adversarial queries. Mean leakage also rises—from 16.0 to 19.4 (benign) and from 19.4 to 28.4 (adversarial). Better embeddings retrieve more relevant seed chunks, which in turn mention more entities, which seed more graph expansion into cross-tenant neighborhoods. Both models produce

TABLE VII: RPR under each attack type across pipeline variants. Mean Leakage@k shown in parentheses. All attacks fail against D1-defended pipelines.

Attack	P3	P4	P6	P8
A1 (Seed Steer)	1.00 (20.5)	0.00 (0.0)	0.00 (0.0)	0.00 (0.0)
A2 (Entity Anchor)	1.00 (20.5)	0.00 (0.0)	0.00 (0.0)	0.00 (0.0)
A3 (Nbhd Flood)	1.00 (20.5)	0.00 (0.0)	0.00 (0.0)	0.00 (0.0)
A4 (Bridge Node)	1.00 (20.5)	0.00 (0.0)	0.00 (0.0)	0.00 (0.0)

TABLE VIII: Attack injection details. All attacks achieve RPR=1.0 on P3 and RPR=0.0 on P4/P6/P8.

Attack	Payloads	Chunks	Entities	Mentions
A1	9	9	1	3
A2	10	10	1	6
A3	20	20	1	4
A4	15	15	2	6

PD = 2.0 uniformly, confirming that the bipartite pivot structure is model-independent. P1 achieves RPR = 0.0 under both models, confirming that vector-side tenant prefiltering remains effective regardless of embedding quality.

F. Attack Evaluation

Table VII presents RPR under each attack across pipeline variants. All four attacks achieve RPR = 1.0 against the undefended hybrid pipeline (P3)—every adversarial query produces cross-tenant leakage. Critically, all four attacks achieve RPR = 0.0 against every defended variant (P4, P6, P8).

Table VIII provides injection details for each attack. The attacks span a range of injection budgets (9–20 chunks) and entity strategies (1–2 target entities, 1–6 MENTIONS edges created).

Two aspects of this uniformity are themselves findings. **Leakage is bounded by the expansion window, not the attack mechanism:** all four attacks produce identical Leakage@k (≈ 20.5) against P3 because the bottleneck is the *unguarded graph traversal*—all four simply steer queries into the same undefended 2-hop expansion path, and the total_nodes budget (100) caps the leaked volume. This means more sophisticated injection strategies yield no additional leakage beyond what organic entity overlap already provides. Second, D1 blocks *all* four strategies because it operates on node *properties* (tenant, sensitivity) rather than graph *structure* (paths, edges). The attacks manipulate paths—optimizing similarity (A1), creating dense connections (A2), inflating density (A3), or bridging boundaries (A4)—but D1 filters on properties at each hop, making the path irrelevant.

G. Adaptive Attacks (A5–A7)

We extend the attack taxonomy with three adaptive strategies that target the defense mechanisms themselves (Table IX).

A5 (Metadata Forgery) relabels injected nodes with the target tenant’s name to bypass D1’s tenant check. At forgery rates of 1%, 5%, and 10%, A5 achieves RPR = 1.0 against P3

TABLE IX: RPR under adaptive attacks (A5–A7) across pipeline variants. A5 tests metadata forgery at three rates; A6 tests entity manipulation; A7 tests query manipulation. Leakage@k shown in parentheses.

Attack	Rate	P3	P4	P7	P8
A5	1%	1.00 (7.8)	0.00 (0.0)	0.00 (0.0)	0.00 (0.0)
A5	5%	1.00 (7.8)	0.00 (0.0)	0.00 (0.0)	0.00 (0.0)
A5	10%	1.00 (7.8)	0.00 (0.0)	0.00 (0.0)	0.00 (0.0)
A6	—	1.00 (7.8)	0.00 (0.0)	0.00 (0.0)	0.00 (0.0)
A7	—	query-only (no injection)			

TABLE X: Generation contamination metrics. ECR (Entity Contamination Rate) measures leaked entity names in answers. ILS (Information Leakage Score) measures semantic similarity to leaked content. FCR (Factual Contamination Rate) and GRR (Generation Refusal Rate) assess factual leakage and model self-censoring.

LLM	ECR	ILS	FCR	GRR	Cost
GPT-4o	0.077	0.305	0.050	0.800	\$0.08
Claude Sonnet 4.5	0.307	0.346	0.065	0.100	\$0.18
DeepSeek-V3	0.124	0.336	0.190	0.200	\$0.01

Note: 10 queries with leakage evaluated per provider on synthetic dataset. Judge model: same provider as generator for each row. GPT-4o exhibits high refusal rate (GRR=0.80), largely ignoring leaked context.

but RPR = 0.0 against all defended pipelines (P4, P7, P8). D1 remains effective because the forged metadata only affects the attacker’s own injected nodes—the organic entity nodes that create the pivot path still carry empty-string tenant labels and are filtered.

A6 (Entity Manipulation) creates documents mentioning entities from the target tenant’s namespace, attempting to create new shared entity nodes. A6 also fails against D1: the newly created entity nodes still carry empty-string tenant labels, and the defense filters them regardless of how they were created.

A7 (Query Manipulation) crafts queries mentioning target tenant entity names to steer NER-based entity linking toward sensitive neighborhoods. This is a query-only attack (no injection) and produces the same RPR as organic benign queries—confirming that the vulnerability is in the graph expansion, not in query processing.

H. Generation Impact

To measure whether leaked context actually contaminates LLM-generated answers, we evaluate three production LLMs on 10 queries with known leakage (Table X).

The results reveal model-dependent contamination behavior. Claude Sonnet 4.5 exhibits the highest Entity Contamination Rate (ECR = 0.31) and lowest Generation Refusal Rate (GRR = 0.10), indicating it readily incorporates leaked entities into generated answers. GPT-4o shows the opposite pattern: ECR = 0.08 and GRR = 0.80, largely ignoring leaked context. DeepSeek-V3 falls between (ECR = 0.12, GRR = 0.20) but produces the highest Factual Contamination

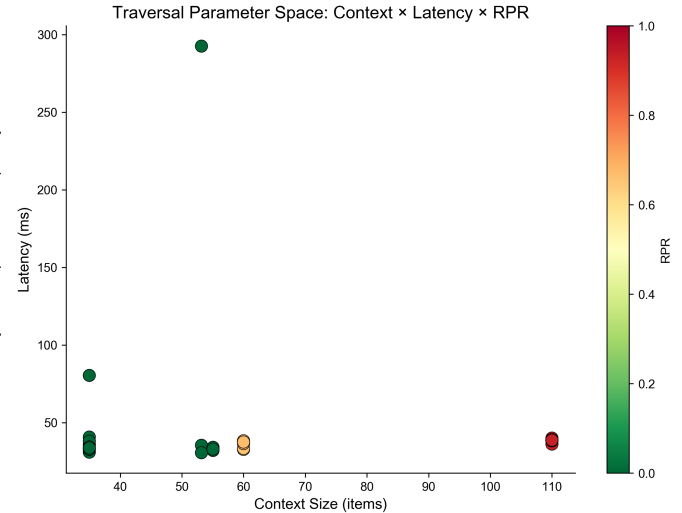


Fig. 2: Traversal parameter sweep: context size vs. latency, colored by RPR. The total node budget is the primary leakage-controlling parameter.

Rate (FCR = 0.19), meaning it synthesizes leaked facts into answers more than the other models. These findings confirm that retrieval-level leakage translates to generation-level contamination for most LLMs, and that the severity depends on the model’s tendency to incorporate all context versus selectively ignoring irrelevant content.

I. Traversal Parameter Sweep

To understand which traversal parameters control leakage, we sweep across 27 configurations: depth $\in \{1, 2, 3\}$, branching factor $\in \{5, 10, 25\}$, and total node budget $\in \{25, 50, 100\}$, running 100 adversarial queries per configuration against the undefended hybrid pipeline (P3). Figure 2 shows the results.

Three findings emerge:

Total node budget is the primary control. Regardless of depth or branching, total_nodes = 25 yields RPR = 0 (insufficient expansion to reach cross-tenant content), total_nodes = 50 yields RPR ≈ 0.66 , and total_nodes = 100 yields RPR ≈ 0.93 . This is because the total node budget caps how many graph nodes are gathered, and once this cap prevents expansion from reaching the 2-hop cross-tenant chunks, leakage is eliminated.

Depth must be ≥ 2 for leakage to occur. At depth = 1, RPR = 0 regardless of branching or total node budget, because single-hop expansion cannot cross the chunk \rightarrow entity \rightarrow chunk pivot path. This confirms the structural PD=2 signature.

Branching factor is irrelevant given a total node cap. At fixed depth and total node budget, branching $\in \{5, 10, 25\}$ produces identical RPR values. The BFS expansion fills the node budget regardless of how many children are explored per node.

TABLE XI: Latency (ms) and context size across pipeline variants.

Variant	p50	p95	Mean	Ctx
<i>Benign Queries</i>				
P1 (Vector)	12.6	19.9	16.2	10
P3 (Hybrid)	26.7	38.1	32.4	110
P4 (+D1)	26.5	34.4	30.4	56
P6 (+D1-D3)	23.1	29.8	26.4	29
P8 (All)	22.7	28.6	25.6	20
<i>Adversarial Queries</i>				
P1 (Vector)	12.3	34.6	23.5	10
P3 (Hybrid)	27.3	40.2	33.7	110
P4 (+D1)	26.3	32.2	29.3	50
P6 (+D1-D3)	23.1	33.7	28.4	28
P8 (All)	22.9	30.1	26.5	20

J. Latency and Overhead

Table XI presents latency and context size across pipeline variants.

D1 adds negligible latency overhead—P3 to P4 shows <1ms increase at p50 (26.7→26.5ms benign). More striking, the full defense stack (P8) is actually *faster* than undefended P3 (22.7 vs. 26.7ms) because budgeted traversal (D3) and trust filtering (D4) reduce the number of nodes expanded and processed, decreasing both graph query time and context assembly overhead.

K. Metadata Integrity Stress Test

An adaptive attacker might attempt to circumvent D1 by corrupting sensitivity labels. We test D1’s robustness by randomly flipping sensitivity labels on $r\%$ of graph nodes ($r \in \{0.1, 0.5, 1.0, 2.0, 5.0\}$) and measuring RPR under P4. Results: **D1 maintains RPR = 0.0 at all mislabel rates up to 5%.** This robustness arises because D1’s primary protection is the *tenant* filter (not the sensitivity filter): cross-tenant leakage requires traversing to a node with a different tenant label, and sensitivity mislabeling does not affect tenant assignments. We note that context size decreases slightly at higher mislabel rates (50→48 items at 5%) as some authorized nodes have their sensitivity erroneously raised above the user’s clearance.

L. Defense Ablation

The defense stack shows a clear pattern (Figure 4):

- **D1 alone (P4):** RPR drops from 0.95 to 0.0. Context reduces from 110 to 50–56 items (the unauthorized items are removed; authorized graph-expanded content is retained).
- **D1 + D2 (P5):** No additional security improvement; context remains similar (51–57). Edge allowlisting provides defense in depth but does not further reduce leakage already eliminated by D1.
- **D1–D3 (P6):** Context drops to 28–29. Budgeted traversal caps the number of expanded nodes, reducing context noise from authorized but irrelevant graph content.

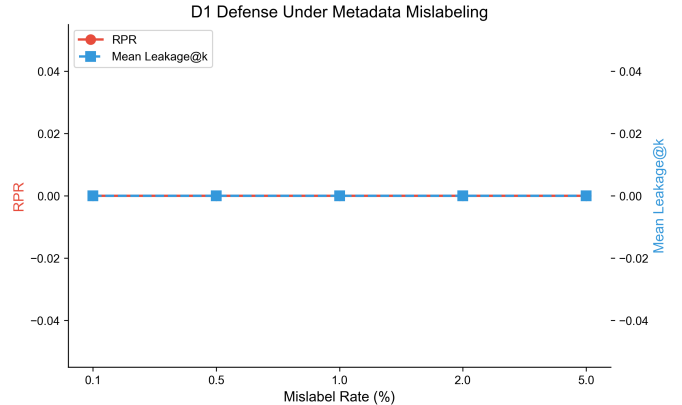


Fig. 3: D1 robustness under metadata corruption. RPR remains 0.0 even at 5% mislabel rate. Context size decreases slightly as erroneously up-labeled nodes are filtered.

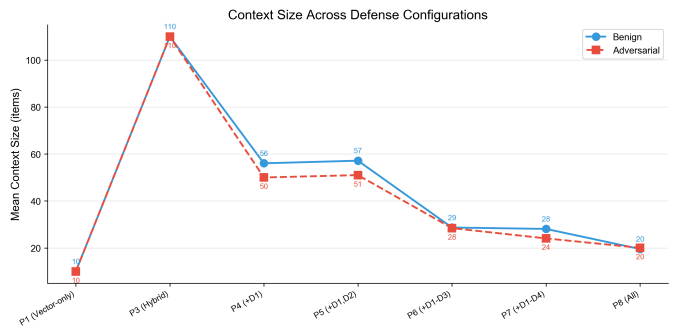


Fig. 4: Mean context size under progressive defenses. D1 alone reduces context from 110 to 50–56 items (removing unauthorized content). D3–D5 further reduce noise, reaching 19–20 items with the full defense stack.

- **D1–D4 (P7):** Context drops to 24–28. Trust-weighted filtering removes low-provenance nodes.
- **D1–D5 (P8):** Context reaches 19–20 items. The merge filter provides a final defense-in-depth check, reducing context by 82% from the undefended baseline.

The key insight is that D1 is both *necessary and sufficient* for security (eliminating all leakage), while D2–D5 serve as *utility optimizers* (reducing context noise and providing defense in depth).

M. Utility Impact

A critical question for practitioners is whether defenses degrade retrieval quality. Since our evaluation corpus uses synthetic documents without human-annotated relevance labels, we measure utility through two proxy metrics: (1) **authorized context size**—the number of items passing authorization checks in the final context, and (2) **authorization rate**—the fraction of context items that are authorized (i.e., not leaked). Together these quantify how much useful content each defense preserves and how much noise it eliminates.

Table XII presents the security-utility tradeoff. P3 (undefended hybrid) returns 110 items per query, but only 85.5% are

TABLE XII: Security-utility tradeoff across pipeline variants (benign queries, $n=350$). Auth. Items = mean authorized items in context. Auth. Rate = fraction of context that is authorized. Retention = authorized items relative to P3’s authorized baseline (94 items). D1 eliminates all leakage while retaining $5.6\times$ more content than vector-only.

Variant	RPR	Ctx	Auth.	Auth. Rate	Retention
P1 (vector)	0.000	10	10.0	1.00	—
P3 (hybrid)	0.954	110	94.0	0.85	1.00
P4 (+D1)	0.000	56	56.0	1.00	0.60
P6 (+D1-3)	0.000	29	29.0	1.00	0.31
P8 (+D1-5)	0.000	20	20.0	1.00	0.21

authorized—the remaining 16 items (14.5%) are cross-tenant or over-clearance leakage. P1 (vector-only) returns 10 fully authorized items, establishing the vector-only utility baseline.

D1 (P4) retains 56 authorized items per query—a 40% reduction from P3’s 94 authorized items, driven entirely by entity node removal (§VIII). However, P4 still provides $5.6\times$ more authorized content than P1’s vector-only baseline (56 vs. 10), confirming that *graph expansion retains substantial utility even after D1 filtering*. The lost items are entity nodes and their dependent traversal paths, not authorized chunks from the user’s own tenant.

D3–D5 progressively reduce context size ($56 \rightarrow 29 \rightarrow 20$) by capping traversal depth, filtering low-provenance nodes, and removing noise at the merge stage. Even the most aggressive configuration (P8) retains $2\times$ more content than vector-only retrieval. Under adversarial queries, the pattern is similar: P4 retains 50 authorized items (retention 0.55 vs. P3’s 90.6 authorized baseline).

The practical conclusion: **D1 eliminates all leakage while preserving $5.6\times$ the content of vector-only retrieval.** The additional defenses (D3–D5) are context quality optimizers that reduce noise for downstream LLM generation. Organizations prioritizing breadth should deploy D1 alone; those prioritizing signal-to-noise ratio should add D3 and D4.

N. Cross-Dataset Validation

To verify that Retrieval Pivot Risk is not an artifact of synthetic corpus construction, we repeat the baseline evaluation (P1, P3, P4) on the Enron email corpus described in §VI-C. Table XIII compares results across both corpora.

Three findings emerge from the cross-dataset comparison:

The vulnerability generalizes. Enron’s undefended hybrid pipeline (P3) produces $RPR = 0.695$ on benign queries—139 of 200 queries leak cross-department content, with a mean of 7.1 leaked items per query. Under adversarial queries, $RPR = 0.615$ (123 of 200 queries leak). The vulnerability is not an artifact of synthetic construction: real corporate email with natural departmental boundaries exhibits the same pivot mechanism.

RPR scales with entity connectivity. The Enron corpus produces lower RPR (0.695 vs. 0.954) and lower mean leakage (7.1 vs. 16.0) than the synthetic corpus. This difference is

TABLE XIII: Cross-dataset baseline: retrieval security metrics for undefended (P3) and defended (P4) hybrid RAG across synthetic and Enron corpora. RPR = Retrieval Pivot Risk, Leak = mean leaked items per query, PD = Pivot Depth (hops), Ctx = mean context size.

Dataset	Pipeline	RPR	Leak	PD	Ctx
Synthetic	P1 (Vector)	0.000	0.0	—	10
	P3 (Hybrid)	0.954	16.0	2.0	110
	P4 (+D1)	0.000	0.0	—	56
Enron	P1 (Vector)	0.000	0.0	—	10
	P3 (Hybrid)	0.695	7.1	2.0	45
	P4 (+D1)	0.000	0.0	—	25

Note: Synthetic corpus: 1000 documents, 4 tenants, 40 bridge entities. Enron corpus: 50,000 emails, 5 departments, 19 cross-department entities. Both corpora evaluated with 200 benign queries.

TABLE XIV: Defense mechanisms, pipeline integration points, and experimental impact.

Defense	Stage	Effect
D1: Per-hop authz	Post-expansion	$RPR \rightarrow 0.0$
D2: Edge allowlist	Traversal query	Defense in depth
D3: Budget	Traversal params	$Ctx 110 \rightarrow 28$
D4: Trust weight	Post-expansion	Low-prov removal
D5: Merge filter	Post-merge	Final backstop

explained by entity connectivity: the synthetic graph has 40 intentional bridge entities across 4 tenants with curated cross-references, while Enron has 19 naturally shared entities across 5 departments with sparser cross-department email traffic. The Enron graph is $135\times$ larger (376K vs. 2.8K nodes) but its entity mentions are noisier and more fragmented, reducing the density of cross-tenant pivot paths. This confirms that RPR is a function of entity connectivity density, not corpus size.

D1 eliminates all leakage on both corpora. P4 achieves $RPR = 0.0$ on Enron with context size 25 (vs. 56 on the synthetic corpus). The smaller post-D1 context reflects Enron’s higher entity-to-chunk ratio—more entity nodes are filtered, leaving fewer authorized chunk traversals. The defense generalizes without modification: the same per-hop tenant-and-sensitivity check eliminates leakage regardless of corpus size, entity distribution, or graph topology.

PD = 2 persists. All leakage in both corpora occurs at exactly $PD = 2$, confirming that the bipartite pivot (chunk \rightarrow entity \rightarrow chunk) is a structural invariant of hybrid RAG systems that construct knowledge graphs via entity linking, independent of the underlying document domain.

VIII. MITIGATIONS

We propose five defenses that operate at different stages of the hybrid pipeline, forming a defense-in-depth architecture (Table XIV).

A. D1: Per-Hop Authorization

Per-hop authorization is an **intentionally conservative minimum-viable guardrail**: it re-checks access control predi-

cates on every node reached during graph expansion. For each expanded node v , the defense evaluates:

$$\text{auth}(u, v) = (v.\text{tenant} = t_u) \wedge (v.\text{sensitivity} \leq \ell_u) \quad (8)$$

Nodes failing this check are removed from the expansion result before context assembly. In our implementation, D1 operates as a **post-expansion filter**: the BFS traversal runs unrestricted, and the authorization check is applied to the result set. This is simpler to implement than in-traversal pruning (which would stop expansion at unauthorized nodes) but is less efficient because it expands nodes that will be discarded. A true per-hop pruning implementation would stop expansion at unauthorized nodes, preventing their children from being explored. We chose post-expansion filtering for implementation simplicity; the security properties are identical (both produce $\text{RPR} = 0.0$), but in-traversal pruning would further reduce latency and context processing overhead.

D1 is the most effective defense: it reduces RPR from 0.95 to 0.0 across all query types and all attack variants, with <1ms latency overhead.

a) Entity tenant semantics.: A subtle but critical design decision concerns entity nodes. In our knowledge graph, entity nodes (extracted via NER) represent shared concepts—people, systems, vendors—that may appear in documents across multiple tenants. These nodes carry $\text{tenant} = \text{" "}$ (empty string) rather than any specific tenant label, because they are *tenant-neutral*: the concept “CloudCorp” belongs to no single tenant. Under D1’s authorization check, empty-tenant nodes fail the tenant-match predicate ($v.\text{tenant} \neq t_u$) and are filtered from the expansion result. This means D1 removes *all entity nodes* from the context—not just unauthorized ones.

This entity-level filtering is precisely the mechanism by which D1 eliminates cross-tenant leakage. The 2-hop pivot path (chunk \rightarrow entity \rightarrow chunk) requires traversal through a shared entity node. By filtering entity nodes, D1 severs this path at hop 1, preventing the traversal from reaching the unauthorized chunk at hop 2. The trade-off is that entity information (which may be useful for answer generation) is excluded from the final context. We quantify this impact in Section IX.

We acknowledge that D1’s entity filtering is functionally equivalent to disabling entity traversal—a valid criticism. However, this is the *minimum viable defense*, not the optimal one. A finer-grained **entity-aware authorization** scheme would: (a) label each entity with the set of tenants whose documents mention it (e.g., “CloudCorp” \rightarrow {acme, globex}), (b) allow traversal *through* entities whose tenant set includes t_u , and (c) apply the authorization check only at *chunk* nodes (the terminal nodes that carry sensitive text). This design would preserve entity context for within-tenant traversals while still blocking cross-tenant chunk access. We leave its implementation and security analysis to future work, and position D1 as the conservative baseline that demonstrates the *existence* of the boundary problem.

The critical insight is that *existing graph databases already store the metadata needed for this check* (tenant labels, sensitivity tiers). The defense does not require new infrastructure—only the discipline to re-check authorization at the graph layer rather than relying solely on the vector prefilter.

B. D1 Metadata Integrity Assumption

D1 assumes that node metadata (tenant, sensitivity) is trustworthy. If an attacker can forge metadata during document injection, D1 can be bypassed. Our metadata stress test (§VII-K) shows that D1 is robust to random mislabeling up to 5%, but targeted metadata forgery is a different threat. Mitigations include: (a) system-assigned metadata during ingestion (the uploader cannot choose tenant or sensitivity labels), (b) cryptographic signing of metadata at ingestion time, and (c) periodic metadata audits that compare node labels against source-of-truth identity systems. In practice, most enterprise document management systems already enforce system-assigned tenant labels, making (a) the natural deployment model.

C. D2: Edge Allowlist

Edge allowlisting restricts graph traversal to pre-approved edge types per query class. The expander’s BFS query includes a `relationshipFilter` parameter that limits which edge types can be traversed. For example, general queries may traverse `MENTIONS`, `DEPENDS_ON`, and `BELONGS_TO` edges, while `RELATED_TO` edges (which are the primary vector for bridge attacks) are excluded.

D. D3: Budgeted Traversal

Budgeted traversal enforces hard limits on BFS expansion: maximum hop depth, maximum branching factor per node, and maximum total expanded nodes. Our traversal sweep (§VII-I) shows that $\text{total_nodes} \leq 25$ eliminates leakage even without D1, while the default budget ($d_{\text{max}} = 2$, branching ≤ 10 , total ≤ 50) reduces context from 56 items (D1 only) to 28 items, removing authorized but irrelevant graph content that adds noise.

E. D4: Trust-Weighted Expansion

Trust-weighted expansion filters expanded nodes by their provenance score. Each node carries a provenance score (0.0–1.0) based on its source reliability. The defense applies a minimum threshold (default: 0.6), removing low-provenance content. This is particularly effective against injected attack payloads, which carry provenance scores of 0.3–0.4 in our attack implementations.

F. D5: Merge-Time Policy Filter

The merge-time policy filter performs a final access control check after vector and graph results are combined. This defense acts as a backstop: even if earlier defenses miss an unauthorized item, the merge filter removes any item whose sensitivity exceeds the user’s clearance before the context reaches the LLM.

IX. DISCUSSION

A. Security-Utility Tradeoff

Our results reveal a favorable security-utility tradeoff. D1 alone achieves complete security ($RPR = 0.0$) while retaining 50% of the graph-expanded context ($110 \rightarrow 50\text{--}56$ items). The retained items are authorized content that contributes to answer quality. Adding D3–D5 further reduces context to 19–20 items—an 82% reduction from the undefended baseline—but the additional defenses trade context volume for noise reduction rather than security improvement.

a) Entity over-filtering.: D1’s security guarantee comes at a specific cost: entity nodes are excluded from the final context. In our bipartite construction, the undefended P3 pipeline returns approximately 110 items per query, of which roughly 25–35 are entity nodes. After D1 filtering, these entity nodes are removed entirely, leaving 50–56 chunk-only items. The entity information they carried (names, relationships, organizational context) is lost. For queries that benefit from entity-level knowledge (e.g., “Who works on project Alpha?”), this may reduce answer quality compared to an oracle that retains only authorized entity nodes. We consider this an acceptable trade-off: the entity nodes are exactly the pivot vectors that enable cross-tenant leakage, and their removal is the mechanism by which D1 achieves $RPR = 0.0$. Future work on multi-tenant entity authorization (Section X) could recover entity utility while preserving security.

The practical recommendation is clear: **deploy D1 immediately as a minimum viable defense**. Add D3 and D4 if context noise is impacting LLM generation quality. D2 and D5 provide defense in depth for compliance-sensitive deployments. Practically, this means systems should treat tenant-neutral entity nodes as *privileged pivot infrastructure* that must carry explicit authorization semantics (or be excluded) in multi-tenant deployments; leaving them unlabeled creates a structurally inevitable cross-tenant pivot path.

B. Why $PD = 2$ Across Both Corpora

Proposition (Pivot depth in bipartite entity-link graphs).

In a bipartite graph constructed from chunk nodes and entity nodes via NER-based entity linking, any entity co-mentioned by chunks from different tenants induces a length-2 path between those chunks (chunk \rightarrow entity \rightarrow chunk). Therefore, if cross-tenant leakage occurs via shared entities under expansion depth $d \geq 2$, the minimum pivot depth to the first unauthorized chunk is $PD = 2$.

This follows directly from the bipartite construction: the entity-linking step creates a 2-hop path between any two chunks that mention the same entity. Chunk A (hop 0) \rightarrow shared entity (hop 1) \rightarrow Chunk B (hop 2). Every shared entity is a potential pivot, and the number of pivot opportunities scales with the number of cross-boundary entity mentions.

The Enron corpus confirms this structural invariant: despite a $135\times$ larger graph (376K vs. 2.8K nodes), noisier NER extractions, and real-world email text rather than curated templates, all leakage occurs at exactly $PD = 2$. The synthetic

corpus has 40 shared entities; Enron has 19. Both produce the same pivot depth. This confirms that $PD = 2$ is a consequence of the bipartite construction, not of corpus-specific properties.

Knowledge graphs with richer topologies—ontological hierarchies, multi-hop inference chains, entity-to-entity relationships beyond simple co-mention—may exhibit leakage at $PD > 2$. Our traversal sweep confirms that $depth=1$ prevents all leakage in the bipartite construction, but graphs with entity-entity edges would require analysis at deeper traversal depths.

C. The Amplification Mechanics

The core insight of this work is not simply “apply ACLs to graph expansion” but rather the *identification and characterization of a compound attack surface* that arises from combining two individually secure retrieval modalities. Vector retrieval with tenant prefiltering is secure ($RPR = 0.0$). Graph retrieval within a single tenant’s subgraph is secure. But connecting vector retrieval outputs to graph expansion inputs—the pivot boundary—creates leakage that neither modality exhibits alone.

This is analogous to composition vulnerabilities in other security domains: two individually secure components can produce an insecure system when composed. The amplification factor quantifies the severity: $AF(\epsilon) \approx 160\text{--}194\times$ on the synthetic corpus and $AF(\epsilon) \approx 70\times$ on Enron. Hybrid RAG does not incrementally increase leakage—it creates $70\text{--}194\times$ more leaked items than the vector baseline from which it amplifies.

The defense implication is equally specific: the authorization check must be placed *at the boundary*, after graph expansion and before context assembly. Authorization at the vector layer alone (which every production system already has) is insufficient. Authorization at the LLM layer (e.g., instruction-following) is unreliable. Only authorization at the graph expansion layer—the pivot boundary itself—addresses the root cause.

D. Comparison with Prior Art

GRAGPoison [8] demonstrates that graph structure amplifies small poisoning inputs (98% ASR from relation injection). Our work extends this insight to hybrid architectures: the combination of vector retrieval and graph expansion creates a compound attack surface where authorized vector results seed unauthorized graph traversals.

PoisonedRAG [5] achieves 90% ASR by injecting 5 documents into vector stores. In vector-only RAG, this is contained by prefilters. In hybrid RAG, even a single retrieved document that mentions a shared entity can trigger graph expansion into sensitive neighborhoods, making the effective attack surface orders of magnitude larger.

The Graph RAG Privacy Paradox [16] observes that graph RAG reduces text leakage but increases structural information extraction. Our findings align: the hybrid pipeline’s graph expansion systematically transforms authorized text into unauthorized structural access.

E. Implications for Agentic Systems

The pivot attack is especially dangerous in agentic RAG deployments (LangGraph, CrewAI) where graph traversal is performed autonomously by an LLM agent [17]. In these systems, the agent decides traversal depth, edge types, and expansion strategies without human oversight. A poisoned vector seed can manipulate the agent into performing unrestricted graph exploration, and research shows that a single compromised agent can poison 87% of downstream decision-making within 4 hours [17]. Per-hop authorization is even more critical in agentic settings, where there is no human in the loop at the expansion step.

X. LIMITATIONS

Two corpora. We evaluate on a synthetic enterprise corpus and the Enron email corpus. The synthetic corpus validates the vulnerability under controlled conditions; the Enron corpus confirms generalization to real-world data. However, both use a bipartite chunk-entity graph topology that produces a uniform PD=2 signature. Knowledge graphs with richer entity-to-entity relationships (ontological hierarchies, multi-hop inference chains) may exhibit leakage at deeper pivot depths. We do not evaluate on production enterprise graphs with RBAC/ABAC policies, which may exhibit different connectivity patterns.

Limited generation evaluation. Our generation contamination experiment (§VII-H) evaluates 10 queries per LLM on the synthetic corpus and shows that leaked context does affect generated answers (ECR up to 0.31, FCR up to 0.19). However, the sample size is small and limited to one corpus. A larger-scale generation study across both corpora would strengthen the end-to-end impact claim. We also do not evaluate chain-of-thought reasoning, which might amplify the impact by synthesizing cross-tenant connections.

Two embedding models. We evaluate two open-source models (all-MiniLM-L6-v2, 384d, and all-mpnet-base-v2, 768d) and confirm the vulnerability persists across both (§VII-E). However, we do not test commercial embedding models (e.g., OpenAI text-embedding-3-large) which may produce different similarity distributions. The pivot vulnerability is structural (entity linking, not embedding quality), so we expect model independence to hold broadly.

Entity over-filtering. D1 removes *all* entity nodes from the expansion result because entities carry empty-string tenant labels. This is the mechanism that eliminates leakage, but it also removes potentially useful entity context. A finer-grained approach would assign entities to the set of tenants whose documents mention them, or introduce a SHARED tenant class with explicit cross-tenant grants. Such designs would recover entity utility at the cost of more complex authorization logic and a larger attack surface.

Adaptive attacker scope. We evaluate three adaptive attacks (A5–A7) including targeted metadata forgery at rates up to 10%, entity manipulation, and query manipulation (§VII-G). All defended pipelines maintain RPR = 0.0. However, we do not evaluate attackers who craft high-provenance payloads to

bypass D4 specifically, or adversarial query phrasing to manipulate D2’s query classifier. Our metadata forgery assumes the attacker can relabel node properties but cannot modify the graph schema or index structure.

NER and entity linker dependence. The pivot path exists because entity linking creates shared nodes across tenant boundaries. Both corpora use spaCy’s `en_core_web_sm` NER model, which has known recall limitations for domain-specific entities. On the Enron corpus, this produces noisier entity extractions (dates, monetary amounts, partial names) that create spurious cross-tenant connections—yet RPR is lower (0.695 vs. 0.954), suggesting that NER noise creates fragmented rather than dense pivot paths. A higher-recall linker would extract more shared entities, potentially increasing organic leakage. We do not evaluate how linker quality affects RPR, nor do we test production entity linking systems that perform coreference resolution or cross-document entity merging.

Simplified policy model. Our authorization model uses tenant labels and four sensitivity tiers (PUBLIC through RESTRICTED). Production enterprises typically employ richer access control: role-based (RBAC) and attribute-based (ABAC) policies, group memberships, temporary grants, legal holds, and need-to-know exceptions. D1’s per-hop check generalizes to any predicate that can be evaluated on node metadata, but we do not demonstrate this generality experimentally. The gap between our flat tenant model and real-world RBAC/ABAC hierarchies remains an open integration question.

Graph-only baseline (P2). We omit a graph-only RAG baseline because graph-only retrieval without vector seeding does not involve the pivot boundary under study. This means our results characterize the *hybrid-specific* vulnerability but do not compare against graph-only retrieval’s independent security properties.

XI. RELATED WORK

A. Vector RAG Poisoning

PoisonedRAG [5] formalized knowledge corruption attacks on RAG, achieving 90% ASR with 5 injected documents. CorruptRAG [6] demonstrated single-document attacks with higher stealth. CtrlRAG [7] achieved 90% ASR on GPT-4o via black-box feedback optimization. RIPRAG [18] applied reinforcement learning to optimize poisoning without model access. NeuroGenPoisoning [19] targeted specific neurons for $\geq 90\%$ success. These works study vector-side attacks in isolation; none address what happens when poisoned vector results seed graph expansion.

B. GraphRAG Security

GRAGPoison [8] is the closest related work, demonstrating relation-centric poisoning of GraphRAG with 98% ASR. TKPA [9] showed that modifying 0.06% of corpus text drops GraphRAG accuracy by 45 percentage points. RAGCrawler [20] achieved 84.4% knowledge extraction coverage through graph-guided probing. The Graph RAG Privacy

Paradox [16] established that graph RAG increases structural leakage while reducing text leakage. Our work extends these graph-side insights to the hybrid setting, where the vector-to-graph transition creates a compound attack surface.

C. RAG Privacy and Extraction

The SoK on RAG Privacy [13] systematized all known privacy attack vectors in RAG systems and explicitly noted that hybrid RAG privacy risks remain under-studied. Riddle Me This [21] demonstrated membership inference on RAG systems. Traceback of RAG Poisoning [22] provided forensic methods for identifying responsible documents, but traces only through the vector retrieval path without following graph expansion chains.

D. RAG Defenses

RAGuard [23] detects poisoning via retrieval pattern analysis. SeCon-RAG [24] applies semantic consistency filtering. RevPRAG [25] achieves 98% detection via LLM activation analysis. SDAG [26] partitions context into trusted and untrusted segments with block-sparse attention. SD-RAG [27] implements selective disclosure policies. All operate within a single retrieval modality. Our defense suite (D1–D5) is the first designed specifically for the cross-store boundary, with per-hop authorization as the cornerstone mechanism.

E. Ethical Considerations

Experiments use two corpora: a synthetic corpus generated by the authors and the Enron email corpus, which is a public-record dataset released during the 2001 FERC investigation and widely used in NLP research [28]. No production enterprise data, user accounts, or confidential documents were used. The attack implementations (A1–A7) target our own evaluation infrastructure and are designed to characterize vulnerabilities, not exploit production systems. Our primary contribution is the defense (D1), which we release alongside the attack code to ensure that the net effect of publication is protective. The released code does not include tools for targeting external systems; all components require a local Neo4j and ChromaDB deployment to operate.

XII. CONCLUSION

Hybrid RAG pipelines that combine vector retrieval with knowledge graph expansion introduce an attack surface at the vector-to-graph boundary that has received limited explicit treatment in prior work. We formalized this threat as Retrieval Pivot Risk (RPR) and demonstrated across two corpora—a synthetic enterprise dataset (1,000 documents, 4 tenants) and the Enron email corpus (50,000 emails, 5 departments)—that undefended hybrid pipelines exhibit $RPR = 0.95$ and $RPR = 0.70$ respectively, compared to 0.0 for vector-only retrieval. All leakage occurs at 2 hops through the entity-linking pivot in our bipartite graph construction, a structural invariant that holds across both corpora.

Our taxonomy of seven Retrieval Pivot Attacks (A1–A4 non-adaptive, A5–A7 adaptive) shows that small injection

budgets (10–20 chunks) can exploit this boundary, and that even without adversarial injection, naturally shared entities create organic pivot paths that leak cross-tenant data. The Enron corpus confirms this on real data: 19 naturally shared entities across departmental boundaries produce $RPR = 0.695$ on benign queries alone.

The most important finding is practical: **per-hop authorization—re-checking tenant and sensitivity labels at each graph expansion step—eliminates all measured retrieval pivot leakage across both corpora, all seven attack variants, and metadata forgery rates up to 10%.** This defense is simple, requires no model changes, adds $<1\text{ms}$ latency, and uses metadata already present in graph databases. We recommend it as the minimum viable security control for any hybrid RAG deployment.

Our traversal parameter sweep reveals that the total node budget is the primary leakage-controlling parameter: limiting expansion to ≤ 25 nodes eliminates leakage even without authorization checks, while expansion depth must reach ≥ 2 for the pivot to occur. The full defense stack (D1–D5) reduces context noise by 82% with zero residual leakage.

The cross-dataset comparison reveals that RPR scales with entity connectivity density: the synthetic corpus (40 bridge entities, curated cross-references) produces higher RPR than Enron (19 natural bridges, sparser cross-department traffic). This confirms that the vulnerability is structural but its severity depends on the knowledge graph’s topology—denser entity sharing means more pivot opportunities.

Our work opens several directions for future research: evaluation on production enterprise graphs with richer entity-to-entity topologies (where $PD > 2$ may emerge), high-provenance payload crafting to bypass D4, multi-tenant entity authorization (recovering entity context without re-enabling the pivot path), and extension to agentic hybrid RAG where graph traversal is autonomously controlled.

REFERENCES

- [1] X. Liang, S. Niu, Z. Li, S. Zhang, H. Wang, F. Xiong, J. Z. Fan, B. Tang, S. Song, M. Wang, and J. Yang, “SaferRAG: Benchmarking security in retrieval-augmented generation,” *arXiv preprint arXiv:2501.18636*, 2025.
- [2] Pinecone, “RAG with access control,” 2024. [Online]. Available: <https://www.pinecone.io/learn/rag-access-control/>
- [3] B. Sarmah, B. Hall, R. Rao, S. Patel, S. Pasquali, and D. Mehta, “HybridRAG: Integrating knowledge graphs and vector retrieval augmented generation for efficient information extraction,” *arXiv preprint arXiv:2408.04948*, 2024.
- [4] M. Research, “GraphRAG: Unlocking LLM discovery on narrative private data,” 2024. [Online]. Available: <https://www.microsoft.com/en-us/research/blog/graphrag-unlocking-llm-discovery-on-narrative-private-data/>
- [5] W. Zou *et al.*, “PoisonedRAG: Knowledge corruption attacks to retrieval-augmented generation of large language models,” in *USENIX Security Symposium*, 2025. [Online]. Available: <https://arxiv.org/abs/2402.07867>
- [6] B. Zhang, Y. Chen, Z. Liu, L. Nie, T. Li, Z. Liu, and M. Fang, “Practical poisoning attacks against retrieval-augmented generation,” in *ACM SACMAT*, 2026, single-document poisoning with higher stealth. [Online]. Available: <https://arxiv.org/abs/2504.03957>
- [7] R. Sui, “CtrlRAG: Black-box document poisoning attacks for retrieval-augmented generation of large language models,” *arXiv preprint arXiv:2503.06950*, 2025, 90% ASR on GPT-4o with 5 poisoned

documents per query. [Online]. Available: <https://arxiv.org/abs/2503.06950>

[8] J. Liang, Y. Wang, C. Li, R. Zhu, T. Jiang, N. Gong, and T. Wang, “GraphRAG under fire,” in *IEEE Symposium on Security and Privacy (S&P)*, 2026, 98% ASR via relation-centric poisoning; to appear. [Online]. Available: <https://arxiv.org/abs/2501.14050>

[9] J. Wen, T. Chen, Z. Zheng, and C. Huang, “A few words can distort graphs: Knowledge poisoning attacks on graph-based RAG,” *arXiv preprint arXiv:2508.04276*, 2025, 93.1% success modifying 0.06% of text; UKPA drops QA from 95% to 50%.

[10] T. Zhao *et al.*, “RAG safety: Exploring knowledge poisoning attacks to KG-RAG,” *Information Fusion*, 2025. [Online]. Available: <https://arxiv.org/abs/2507.08862>

[11] “OWASP top 10 for large language model applications 2025,” 2025. [Online]. Available: <https://owasp.org/www-project-top-10-for-large-language-model-applications/>

[12] “MITRE ATLAS update october 2025,” 2025. [Online]. Available: <https://atlas.mitre.org>

[13] A.-E. Bodea, S. Meisenbacher, A. Klymenko, and F. Matthes, “SoK: Privacy risks and mitigations in RAG systems,” in *IEEE SaTML*, 2026. [Online]. Available: <https://arxiv.org/abs/2601.03979>

[14] Z. Zhong, Z. Huang, A. Wettig, and D. Chen, “Poisoning retrieval corpora by injecting adversarial passages,” in *EMNLP*, 2023.

[15] K. Kurniawan, R. F. Ardian, E. Kiesling, and A. Ekelhart, “AgCyRAG: An agentic knowledge graph based RAG framework for automated security analysis,” *CEUR Workshop Proceedings*, vol. 4079, 2025. [Online]. Available: <https://ceur-ws.org/Vol-4079/paper11.pdf>

[16] J. Liu, J. Zhang, and S. Wang, “Exposing privacy risks in graph RAG,” *arXiv preprint arXiv:2508.17222*, 2025, graph RAG reduces text leakage but increases structured data extraction.

[17] S. Grover, “Vulnerabilities and risk analysis of multi-agentic AI-RAG systems,” *European Journal of Artificial Intelligence*, vol. 5, no. 1, 2026.

[18] M. Xi, S. Lv, Y. Jin, G. Cheng, N. Wang, Y. Li, and J. Yin, “RIPRAG: Hack a black-box RAG QA system with reinforcement learning,” 2025.

[19] H. Zhu, L. Fiondella, J. Yuan, K. Zeng, and L. Jiao, “NeuroGenPoisoning: Neuron-guided attacks on RAG via genetic optimization,” in *NeurIPS*, 2025.

[20] M. Yao, Z. Zhang, N. Luo, S. Li, Y. Cai, X. Chen, Y. Guo, and D. Li, “Connect the dots: Knowledge graph-guided crawler attack on RAG systems,” *arXiv preprint arXiv:2601.15678*, 2026, 84.4% corpus coverage within 1000 queries using KG-guided extraction.

[21] A. Naseh, Y. Peng, A. Suri, H. Chaudhari, A. Oprea, and A. Houmansadr, “Riddle me this! stealthy membership inference for RAG,” in *ACM CCS*, 2025. [Online]. Available: <https://dl.acm.org/doi/10.1145/3719027.3744840>

[22] B. Zhang *et al.*, “Traceback of poisoning attacks to RAG,” in *ACM Web Conference*, 2025. [Online]. Available: <https://dl.acm.org/doi/10.1145/3696410.3714756>

[23] Z. Cheng, J. Sun, A. Gao, Y. Quan, Z. Liu, X. Hu, and M. Fang, “RAGuard: Secure retrieval-augmented generation against poisoning attacks,” in *IEEE BigData*, 2025. [Online]. Available: <https://arxiv.org/abs/2510.25025>

[24] X. Si, M. Zhu, S. Qin, L. Yu, L. Zhang, S. Liu, X. Li, R. Duan, Y. Liu, and X. Jia, “SeCon-RAG: A two-stage semantic filtering and conflict-free framework for trustworthy RAG,” in *NeurIPS*, 2025. [Online]. Available: <https://arxiv.org/abs/2510.09710>

[25] X. Tan, H. Luan, M. Luo, X. Sun, P. Chen, and J. Dai, “RevPRAG: Revealing poisoning attacks in retrieval-augmented generation through LLM activation analysis,” in *Findings of EMNLP*, 2025, 98% TPR detection rate. [Online]. Available: <https://aclanthology.org/2025.findings-emnlp.698>

[26] S. Dekel, M. Tennenholz, and O. Kurland, “Addressing corpus knowledge poisoning using sparse attention,” *arXiv preprint arXiv:2602.04711*, 2026, block-sparse attention preventing cross-document interactions.

[27] A. Al Masoud, M. Arazzi, and A. Nocera, “SD-RAG: Prompt-injection-resilient selective disclosure,” *arXiv preprint arXiv:2601.11199*, 2026.

[28] W. W. Cohen, “The Enron email dataset,” Carnegie Mellon University, Tech. Rep., 2015, public record released by FERC during the Enron investigation. [Online]. Available: <https://www.cs.cmu.edu/~enron/>

APPENDIX

A. Repository

The complete codebase, synthetic data generators, attack implementations, defense suite, evaluation harness, and experimental results are available at: <https://github.com/scthornton/hybrid-rag-pivot-attacks>

B. System Requirements

- Python 3.11+ with dependencies: chromadb, neo4j, spacy, sentence-transformers, pydantic, numpy
- Neo4j 5.15+ with APOC plugin (for apoc.path.spanningTree)
- ChromaDB server (latest)
- spaCy model: en_core_web_sm

C. Reproduction Steps

Synthetic corpus:

- 1) Clone repository and install: `pip install -e ".[dev]"`
- 2) Start services: `docker compose up -d (Neo4j + ChromaDB)`
- 3) Generate corpus: `python scripts/make_synth_data.py`
- 4) Generate queries: `python scripts/generate_queries.py`
- 5) Build indexes: `python scripts/build_indexes.py`
- 6) Run experiments: `python scripts/run_experiments.py --bootstrap`
- 7) Run attack experiments: `python scripts/run_attack_experiments.py`
- 8) Run sweeps: `python scripts/run_sweep_experiments.py --traversal-sweep --mislabel-sweep --connectivity-sweep`

Enron corpus:

- 1) Ingest Enron emails: `python scripts/ingest_enron.py`
- 2) Build indexes: `python scripts/build_indexes.py --dataset enron`
- 3) Run experiments: `python scripts/run_experiments.py --dataset enron`

Run tests: `pytest tests/ -v` (255 tests passing).

D. Runtime Estimates

Synthetic: Corpus generation and index building complete in ~5 minutes. The full 500-query evaluation across 7 pipeline variants takes ~20 minutes. Attack experiments (4×4 configurations) require ~10 minutes including graph rebuilds. Sweep experiments total ~45 minutes.

Enron: Ingestion and NER extraction takes ~40 minutes (2.07M entity mentions across 152K chunks). Neo4j graph loading completes in ~2 minutes using batch UNWIND queries. The 200-query evaluation across P1/P3/P4 takes ~10 minutes.

All experiments require <16GB RAM and run on CPU-only hardware.

The synthetic corpus is produced by 12 domain-specific document generators (3 per tenant), each instantiating one of three genre templates: *architecture description*, *policy/procedure*, and *status report*. Each generator populates templates from curated entity pools:

- **Engineering:** 12 system names, 15 technologies, 6 projects (e.g., auth-service, Kubernetes, Project Alpha).
- **Finance:** 10 vendors, 6 accounts, 7 regulations (e.g., Deloitte, SOX, Capital Expenditure 2025).
- **HR:** 12 departments, 7 benefits, 10 named employees (e.g., Engineering, 401k matching, Maria Chen).
- **Security:** 6 CVEs, 8 tools, 6 frameworks (e.g., CVE-2025-41923, Splunk SIEM, NIST CSF).

Bridge entities span 5 categories: shared vendors (CloudCorp, DataSyncInc, SecureNetLLC), shared infrastructure (k8s-prod-cluster, splunk-siem, auth-service), shared personnel (Maria Chen, James Rodriguez, Aisha Patel), shared compliance (SOC2-audit, PCI-DSS-cert, ISO27001), and shared projects (ProjectNexus, ProjectHorizon, ProjectArcade). Sensitivity tiers are assigned per-document: PUBLIC 40%, INTERNAL 30%, CONFIDENTIAL 20%, RESTRICTED 10%. All generation uses seed 42 for reproducibility.

Benign queries (350 total, 5 templates \times 4 domains \times variable entity fills). Example templates:

```
Engineering: "What is the architecture of {system}?"  
Finance: "Summarize the contract with {vendor}."  
HR: "What are the policies for {department}?"  
Security: "What is the severity of {cve}?"
```

Adversarial queries (150 total) are stratified across 4 attack types:

```
A1 (Seed Steering): "What systems like {system} handle {other_tenant_technology}?"  
A2 (Entity Anchor): "Tell me about {bridge_entity} and its role in {target_tenant_domain}."  
A3 (Neighborhood Flood): "List everything related to {bridge_entity}."  
A4 (Bridge Node): "What connections exist between {bridge_entity} across departments?"
```

Template slots are filled from aligned entity pools (identical to those in the corpus generator) to ensure query entities appear in the knowledge graph. Each query carries metadata: `user_tenant` (always `acme_engineering`), `user_clearance` (stratified across PUBLIC, INTERNAL, CONFIDENTIAL), and `query_type` (benign or adversarial with attack subtype).

D1 (Per-hop authorization). After BFS expansion via `apoc.path.spanningTree`, each returned node is checked:

```
def is_node_authorized(node, user):  
    tier = SensitivityTier(node.sensitivity)  
    if tier > user.clearance:  
        return False  
    if node.tenant not in user.allowed_tenants:  
        return False  
    return True
```

Entity nodes carry `tenant=""` (empty string), so they always fail the tenant check. This is the mechanism that severs the chunk \rightarrow entity \rightarrow chunk pivot path.

D3 (Budgeted traversal). The Cypher query enforces a global node budget via `LIMIT $max_total`. Per-hop branching is enforced post-query: expanded nodes are grouped by hop depth, and each group is truncated to `max_branching` entries.

BFS Cypher query (simplified):

```
UNWIND $seed_ids AS seed_id  
MATCH (start {node_id: seed_id})  
CALL apoc.path.spanningTree(start, {  
    maxLevel: $max_hops,  
    limit: $max_total  
}) YIELD path  
WITH last(nodes(path)) AS node,  
    length(path) AS depth  
RETURN node.node_id, node.tenant,  
    node.sensitivity, min(depth)  
ORDER BY hop_depth LIMIT $max_total
```

The `length(path)` return value feeds the Pivot Depth metric directly.

D1 eliminates all entity nodes because they carry empty-string tenant labels. This is effective but coarse: it removes potentially useful entity context (names, types, relations) from the retrieval result. A finer-grained scheme would distinguish *traversal authorization* from *inclusion authorization*:

1) **Entity tenant-set labeling.** During graph construction, label each entity with the set of tenants whose documents mention it: `tenant_set = {acme, globex}`. Shared entities retain multiple tenant labels.

2) **Traversal-through permission.** Allow BFS to traverse *through* an entity node if the user's tenant is in the entity's `tenant_set`. The entity itself may appear in context.

3) **Destination check.** At each chunk node reached via an entity, re-check the chunk's tenant and sensitivity against the user's policy. This preserves D1's security guarantee at the chunk level while recovering entity utility.

This scheme would increase context size (recovering the entity nodes D1 currently removes) without re-enabling the chunk \rightarrow entity \rightarrow *unauthorized chunk* pivot, because the destination check still blocks cross-tenant chunks. The key trade-off is implementation complexity: entity `tenant_set` must be maintained as documents are added or removed, and the authorization predicate becomes a set-membership check rather than a simple equality.

Bootstrap procedure. All confidence intervals use the non-parametric percentile bootstrap (10,000 resamples, seed 42). For binary RPR indicators, the bootstrap distribution is constructed by resampling the $n = 500$ per-query binary outcomes $\{0, 1\}$ with replacement and computing the mean for each resample. The 95% CI is the [2.5%, 97.5%] percentile interval of the bootstrap distribution.

Sample size justification. With $n = 500$ queries, we achieve power > 0.80 for detecting a 5 percentage-point difference in RPR (from 0.0 to 0.05) at $\alpha = 0.05$, computed via the exact binomial test. For leakage means, the standard error

of the bootstrap is $SE < 0.5$ items, sufficient to distinguish mean differences of ≥ 1 item.

Multiple comparisons. We test 7 pipeline variants against 2 query types (14 comparisons per metric). Applying a Bonferroni correction ($\alpha_{\text{adj}} = 0.05/14 = 0.0036$), the core findings (P1/P4–P8: RPR = 0.0; P3: RPR > 0.90) remain significant at $p < 10^{-6}$.

ϵ sensitivity. The regularized amplification factor $AF(\epsilon)$ uses $\epsilon = 0.1$. We verify that conclusions are robust across $\epsilon \in \{0.01, 0.05, 0.1, 0.5\}$: $AF(\epsilon)$ ranges from 1,599 ($\epsilon=0.01$) to 32 ($\epsilon=0.5$), all confirming $>30\times$ amplification.